

# A Link Quality Estimation-based Beamforming Training Protocol for IEEE 802.11ay MU-MIMO Communications

Mun-Suk Kim, Tanguy Ropitault, SuKyoung Lee, Nada Golmie, Hany Assasa, and Joerg Widmer

**Abstract**—The multi-user multiple-input-multiple-output (MU-MIMO) beamforming training (BFT) enables an access point (AP) and multiple stations (STAs) to determine appropriate directional antenna patterns; to this end, the AP transmits multiple action frames to the STAs during the MU-MIMO BFT. However, if the antenna weight vectors (AWVs) are determined to transmit the action frames inefficiently, this could lead to unnecessary transmissions, which could increase the BFT time. To mitigate the signaling overhead, the schemes used in our previous work employed AWVs, which use multiple beams simultaneously to transmit the action frames. Nevertheless, these existing schemes are still adversely affected by redundant transmissions because these schemes overlook the transmit diversity gain obtained from multi-beam concurrent transmission. Therefore, in this study, we propose a novel transmit antenna configuration scheme that mitigates the signaling overhead by considering the transmit diversity of the inter-symbol interference (ISI) channel incurred when multiple beams are used simultaneously. Our proposed scheme determines each candidate AWV using multiple beams and efficiently identifies the STAs within reach of the corresponding multi-beam concurrent transmission. The numerical and simulation results demonstrate that our proposed scheme shortens the BFT time in comparison with existing schemes.

**Index Terms**—MU-MIMO; Beamforming training; IEEE 802.11ay; mmWave.

## I. INTRODUCTION

RECENTLY, the IEEE 802.11 Task Group ay (802.11ay) has defined new physical and medium access control specifications to enhance the wireless networking performance beyond that of its 802.11ad predecessor; these specifications aim to realize rates up to 100 Gbps [1]. A major advancement is the introduction of a downlink multi-user multiple-input-multiple-output (DL MU-MIMO) transmission [2]. The DL MU-MIMO transmission enables an AP to transmit multiple data streams simultaneously to multiple STAs [3]. To this end, the AP defines a set of STAs as an multi-user (MU) group and performs MU-MIMO BFT with this group. The MU-MIMO BFT entails the AP defining one or more subgroups of STAs in the MU group and determining each transmit AWV to be used when performing DL MU-MIMO transmission with each

subgroup; then, the AP transmits, to the STAs in the MU group, information regarding respective receive AWVs to be used when the STAs in each subgroup receive DL MU-MIMO transmission. The IEEE 802.11ay standard specifies the procedure of the MU-MIMO BFT, which comprises subphases for beamforming (BF) setup, training, feedback, and selection, where the AP transmits multiple action frames to STAs in the MU group [2].

During the MU-MIMO BFT, specifically in the subphases in which the AP broadcasts information regarding the setup and selection of the BFT, the AP needs to continue transmitting copies of an action frame until all STAs in the MU group have received the action frame [2], [3]. In the subphase in which the BFT is conducted, the AP transmits one or more action frames in a one-by-one fashion; throughout each action frame, the AP tests a set of candidate transmit AWVs determined to perform DL MU-MIMO transmission with a subgroup of STAs in the MU group [2] that are reachable by transmitting the action frame [4]. The IEEE 802.11ay standard states that the AP should minimize the number of action frames transmitted in the MU-MIMO BFT; however, determining the AWVs used in the transmissions of these action frames, referred to as *transmit antenna configuration*, for mitigating signaling overhead is not specified in the standard and has been left to vendors to address [2].

Ghasempour *et al.* [3] and Zhou *et al.* [5] investigated communication protocols and interfaces for MU-MIMO BFT, such as the formats of the action frames, modulation and coding schemes, and signaling procedures. A recent study by Blandino *et al.* [6] led to the proposal of a multi-user hybrid MIMO scheme, including channel estimation and frequency selective precoding. Other studies [7] and [8] have developed an efficient system that constructs a set of candidate beams to mitigate inter-stream interference. Myers *et al.* [9] proposed a framework for compressive beam alignment using a perfect array-based codebook. Wu *et al.* [10] investigated the beam alignment problem to obtain the optimal beam pair; to this end, they leveraged the inherent correlation structure among beams and prior knowledge of the channel fluctuation. However, these studies did not consider the transmit antenna configuration for action frames transmitted in the MU-MIMO BFT. Instead, the studies, particularly [6]–[8], focused on the optimization problems to obtain maximum stream separability; the studies [9] and [10] attempted to properly configure transmitting and receiving radios while accelerating the beam alignment process. Our previous study [4] introduced transmit antenna

This work was supported by the National Research Foundation of Korea (NRF) grant funded by the Korea government (MSIT). (No. 2019R1A2C1086191)

M. Kim, T. Ropitault, and N. Golmie are with the National Institute of Standards and Technology, Gaithersburg, MD 20899 USA.

S. Lee is with the Department of Computer Science, Yonsei University, Seoul 03722, South Korea (e-mail: sklee@yonsei.ac.kr).

H. Assasa and J. Widmer are with the IMDEA Networks Institute, 28918 Madrid, Spain.

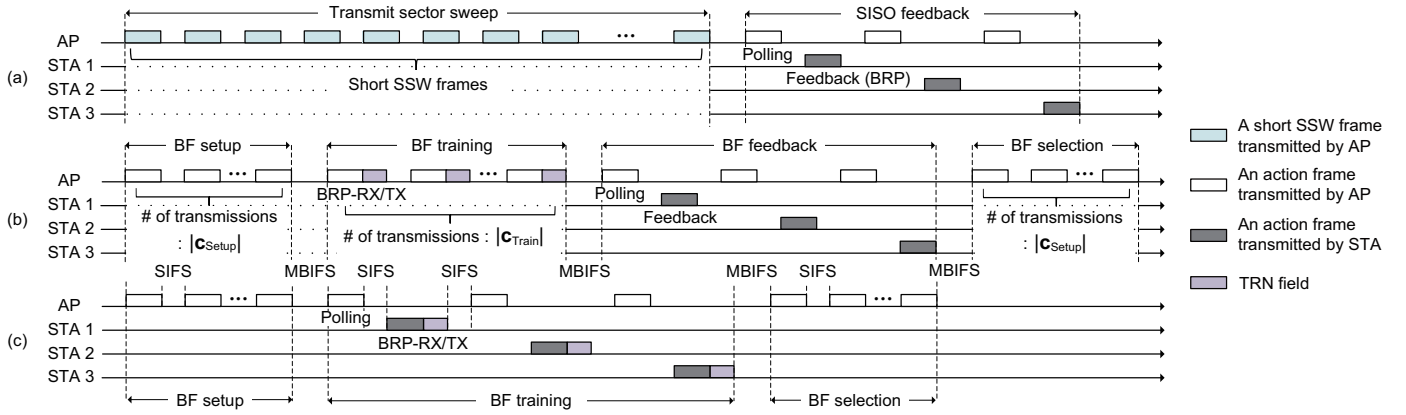


Fig. 1. (a) SISO phase and (b) NRC and (c) RC MIMO phases of the MU-MIMO BFT.

configuration schemes based on the procedures of the MU-MIMO BFT specified in the IEEE 802.11ay standard. The schemes in [4] determined an AWW with which multiple directional beams were simultaneously used to transmit an action frame; however, these schemes overlooked the transmit diversity gain obtained from multiple concurrent beams during the transmission of the action frame.

A practical millimeter wave (mmWave) channel between any two nodes is characterized by a few dominant line-of-sight and reflected non-line-of-sight multipath components [8]. When multiple beams are exploited simultaneously to transmit an action frame, such multipath propagation of each single beam may cause ISI. This causes the AP to be unable to identify STAs within reach of its transmission by using multiple concurrent beams, although it is already aware of the link qualities measured with every single beam; this causes the AP to transmit unnecessary action frames during the MU-MIMO BFT, thereby increasing the BFT time. If the MU-MIMO BFT takes considerable time to establish downlink transmission links between the AP and STAs, the data transmission delay experienced by each STA will be too long to achieve a good quality of experience [5].

To overcome the above problem, in this study, we propose a novel antenna configuration scheme that reduces the signaling overhead by considering the ISI incurred because of the multipath propagation of multiple concurrent beams; the proposed scheme is referred to as the *ISI link quality estimation-based (ILQE) scheme*. The IEEE 802.11ay standard utilizes a transmit diversity technique, cyclic shift diversity (CSD), to transmit action frames for the MU-MIMO BFT. Our ILQE scheme considers the sparse multipath properties of mmWave and the transmit diversity of the ISI channel to estimate the quality of each link that could be used for the simultaneous transmission of each candidate set of multiple beams. Based on the estimated link qualities, our scheme determines an appropriate antenna configuration with the aim of shortening the BFT time by reducing the number of redundant action frames that are transmitted. The major contributions of this study are summarized as follows:

- First, we present an mmWave system model designed to capture the benefit of the transmit antenna diversity. This

system model enables our ILQE scheme to identify more STAs within reach of the transmission of an action frame, in comparison with existing schemes in [4]; hence, our scheme can support the engagement of additional STAs in MU-MIMO BFT and test a larger number of different subgroups of STAs in the MU group for DL MU-MIMO transmission.

- Second, using the estimated link qualities, our ILQE scheme determines the transmit antenna configuration that enables the corresponding transmissions to reach the largest number of STAs in the MU group; it enables our scheme to reduce redundant action frames transmitted during the MU-MIMO BFT.
- Third, to lower the computational complexity, we provide a heuristic method that can significantly reduce the number of times our ILQE scheme estimates the quality of a link used for the simultaneous transmission of a candidate set of multiple beams.
- Fourth, we describe the analytical models we developed to evaluate the performances of our proposed scheme and the existing schemes in terms of the BFT time. In particular, we analyze the probability of failure of the corresponding transmission when a transmit antenna configuration is used to send an action frame. Then, we evaluate the extent to which this transmission failure affects the BFT time.
- Fifth, we present the extensive simulations conducted to validate our analytical model with network simulator (ns-3) and MATLAB. We implemented the sparse multipath environment based on a quasi-deterministic (Q-D) channel model and the procedure of the IEEE 802.11ay-based MU-MIMO BFT by extending the open source code of [11].

The remainder of this paper is organized as follows: Section II briefly explains the signaling procedures for the MU-MIMO BFT and discusses related work. Section III describes our proposed ILQE scheme. Details of the performance analysis of our scheme and existing schemes are presented in Section IV. Section V discusses the numerical and simulation results. Finally, Section VI concludes this paper.

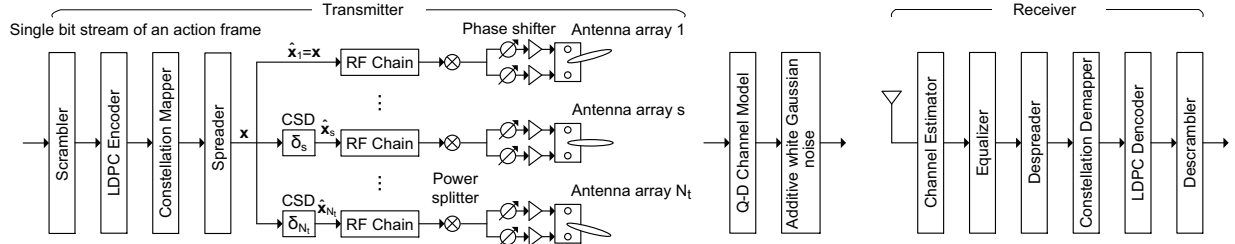


Fig. 2. Simplified hardware block diagram of the transmitter and receiver for control mode transmissions.

## II. BACKGROUND

In this section, we first present the signaling procedure of MU-MIMO BFT. Then, we briefly describe the operation and discuss the limitation of the existing methodologies.

### A. Signaling for MU-MIMO BFT

The MU-MIMO BFT procedure comprises two consecutive phases: single-input-single-output (SISO) and MIMO [3]-[5]. The MIMO phase comprises either a non-reciprocal (NRC) MIMO phase or a reciprocal (RC) MIMO phase. When the AP is equipped with more than one transmit antenna array, each of these arrays can be configured with precomputed AWVs to cover either overlapping or nonoverlapping spatial transmit sectors (TSs).

**SISO phase:** As depicted in Fig. 1(a), the SISO phase starts with a transmit sector sweep, wherein the AP transmits short sector sweep (SSW) frames through different TSs of each of its transmit antenna arrays. The AP collects feedback on its transmit sector sweep from each STA in the MU group. The feedback contains a list of TSs detected when the STA receives the SSW frames and link qualities corresponding to the detected TSs.

**NRC MIMO phase:** It is composed of four subphases, as depicted in Fig. 1(b): BF setup, BF training, BF feedback, and BF selection. First, the AP transmits one or more BF setup frames to STAs in the MU group. The BF setup frame contains information, such as a list of STAs that are engaging in the MIMO phase. Next, in the BF training subphase, the AP transmits one or more beam refinement protocol-receive/transmit (BRP-RX/TX) frames. Each BRP-RX/TX frame includes a training (TRN) field comprising multiple subfields; these subfields are transmitted across candidate transmit AWVs for DL MU-MIMO transmission. Then, each subgroup of STAs in the MU group that has received each BRP-RX/TX frame measure the qualities of respective links on which candidate transmit AWVs have been used. In the BF feedback subphase, each STA in the MU group sends feedback to the AP; this feedback contains a list of candidate transmit AWVs detected when the BRP-RX/TX frames are received. Additionally, the feedback contains the receive antenna array information and measured link qualities corresponding to the detected candidate transmit AWVs. Finally, in the BF selection subphase, the AP announces the subgroups of STAs in the MU group and information regarding the receive antenna array of the STAs in each subgroup that have been designated to conduct DL MU-MIMO transmission.

**RC MIMO phase:** The BF setup and selection subphases operate in the same manner as in the NRC MIMO phase. In the RC BF training subphase, assuming antenna pattern reciprocity, each STA transmits BRP-RX/TX frames and the AP directly measures the link quality of each pair of transmit and receive AWVs, as depicted in Fig. 1(c).

### B. Transmit Antenna Configuration Schemes and their limitation

To the best of our knowledge, our previous study [4] was the first to propose transmit antenna configuration for the MU-MIMO BFT procedure. This study [4] presented two methodologies: largest signal to noise ratio (SNR)-based (LSB) and largest number of reachable STAs-based (LNS). To transmit action frames in the MU-MIMO BFT, the LSB scheme selects the TSs with the largest link qualities, i.e., SNRs, among the TSs known from the SISO feedback of each STA in the MU group, whereas the LNS scheme selects the TSs through which the single-beam transmissions of the AP can reach the largest number of STAs in the MU group.

Both LSB and LNS utilize multiple TSs simultaneously to transmit an action frame. However, these existing schemes determine such multiple TSs based on the qualities of links measured with every single TS; hence, they are unable to consider the transmit diversity of the ISI channel incurred when multiple TSs are used simultaneously. Because of this limitation, these two existing schemes cannot effectively identify STAs in the MU group that are within the reach of an action frame transmitted through multiple TSs simultaneously. This problem leads to performance degradation in the MIMO phase as follows:

- In the subphase of BF setup and selection, the AP repeats the transmission of an action frame with different transmit antenna configurations until it has reached all the STAs engaging in the MIMO phase. However, these existing schemes are likely to perform redundant transmissions to ensure the transmission is received by all the STAs.
- In the NRC BF training subphase, when each action frame is transmitted, the AP sweeps all candidate transmit AWVs throughout the TRN field of the action frame; the candidate transmit AWVs are determined to perform DL MU-MIMO transmission with a subgroup of STAs in the MU group that are within the reach of the action frame to be transmitted. However, both the LSB and LNS schemes are incapable of efficiently identifying all the reachable STAs, given that multiple TSs are selected to transmit

TABLE I  
NOTATIONS FOR THE MODELING AND ANALYSIS OF MU-MIMO BFT

Notation	Description
$N_t$	Number of transmit antenna arrays
$N$	Number of antenna elements used in a transmit antenna array
$T_c$	Single carrier chip time
$\mathbf{h}_s$	Channel vector, which includes the channel coefficients for all delay taps between the $s^{\text{th}}$ transmit antenna array and the receive antenna array
$\delta_{mu}$	SINR threshold, i.e., the minimum SINR that guarantees reliable transmission
$\mathbf{u}_{\text{Tot}}$	Set of all STAs in the MU group
$\mathbf{c}_{\text{Tot}}$	Set of all candidate sets of TSs
$\mathbf{u}_c$	Subgroup of STAs in the MU group that are within the reach of the transmission corresponding to the set $c \in \mathbf{c}_{\text{Tot}}$
$\mathbf{c}_{\text{Setup}}$	Collection of sets of TSs to be used for the transmissions of the BF setup or selection frames
$\mathbf{c}_{\text{Train}}$	Collection of sets of TSs to be used for the transmissions of BRP-RX/TX frames in the NRC BF training subphase
$\mathbf{c}_{\text{poll}}^u$	Set of TSs to be used when transmitting a BF poll frame to STA $u$
$\gamma_{\text{avg}}(u, c)$	Average SINR to be measured at STA $u$ when all TSs of the set $c \in \mathbf{c}_{\text{Tot}}$ are simultaneously used for transmission

the action frame; hence, testing candidate transmit AWWs with all different subgroups of reachable STAs in the MU group may increase the signaling overhead.

To address the aforementioned problems, when determining multiple TSs to transmit an action frame, our proposed ILQE scheme considers the transmit diversity of the ISI channel; then, our ILQE scheme estimates the qualities of the respective links in which candidate sets of multiple TSs, i.e., multiple beams, are used. Based on the qualities of the estimated links, our ILQE scheme can identify STAs within the reach of a candidate set of multiple concurrent beams, although each single beam cannot reach the STAs. This enables our ILQE scheme to shorten the BFT time by reducing the number of unnecessary action frames that are transmitted.

### III. ILQE-BASED TRANSMIT ANTENNA CONFIGURATION FOR MU-MIMO BFT

This section presents the proposed solution for the problem of determining sets of TSs, i.e., precomputed AWWs, to be used to transmit action frames in the MU-MIMO BFT. Fig. 2 illustrates the transceiver architecture as defined by the IEEE 802.11ay standard to transmit the action frames. Fig. 3 depicts the overall procedure of our proposed ILQE scheme. (a) The AP performs the transmit sector sweep of the SISO phase as described in Section II-A. (b) Whenever a short SSW frame is received, each STA in the MU group measures the channel information for the corresponding TS. (c) The AP collects the channel information from each STA in the MU group.

(d) The collected channel information is used to estimate the qualities of respective links for candidate sets of TSs. Our ILQE scheme then selects appropriate sets of TSs to be used for the transmission of action frames in the MU-MIMO BFT.

In this section, we first present an mmWave system model for the MU-MIMO BFT. Next, we explain the method in which each STA estimates the channel information and feeds it back to the AP. Then, we describe the computation of the link qualities for the candidate sets of TSs. Finally, we provide the procedures according to which the appropriate transmit antenna configuration is identified.

Hereinafter, we use the following notations:  $\mathbf{A}$  is a matrix;  $\mathbf{a}$  is a vector,  $\mathbf{a}[l]$  denotes the  $l^{\text{th}}$  value of  $\mathbf{a}$ , and  $|\mathbf{a}|$  denotes the total number of values in  $\mathbf{a}$ ;  $(\cdot)^T$  and  $(\cdot)^*$  denote transpose and conjugate transpose, respectively;  $\lfloor \cdot \rfloor$  denotes the greatest integer less than or equal to a real number, whereas  $\lceil \cdot \rceil$  represents the integer nearest to a real number;  $\|\mathbf{a}\|_p$  is the  $p$ -norm of  $\mathbf{a}$ ;  $\mathbf{I}_N$  is the  $N \times N$  identity matrix.

#### A. System Model

We assume that all action frames in the MU-MIMO BFT are transmitted using the control mode defined in [2] over a 2.16 GHz channel. For ease of exposition, we also assume a sub-connected architecture as in [12], as depicted in Fig. 2, where each radio frequency (RF) chain is connected to only one transmit antenna array; hence, the number of RF chains is the same as that of the transmit antenna arrays. Herein,  $N_t$  and  $N$  denote the number of transmit antenna arrays and the number of antenna elements used in each transmit antenna array, respectively. The bit stream of an action frame is transmitted using multiple RF chains by applying a spatial expansion with CSD; the transmitter, i.e., the AP, maps a single bit stream to all RF chains. The bit stream of each RF chain is finally transmitted through an antenna array associated with the RF chain. The receiver, i.e., each STA, uses a quasi-omni pattern to receive the bit stream.

We consider a frequency selective channel and adopt a block-fading model in which the channel remains unchanged over the transmission block [13]. Let  $\mathbf{h}_s$  and  $h_{s,d}$  denote the channel vector and the channel coefficient for the delay of the  $d^{\text{th}}$  tap in units of  $T_c$ , respectively, between the  $s^{\text{th}}$  transmit and receive antenna arrays. Then, given a transmission block consisting of  $L$  symbols, the channel vector can be defined as follows:

$$\mathbf{h}_s = [h_{s,1}, h_{s,2}, \dots, h_{s,d}, \dots, h_{s,\nu} \dots 0], \quad (1)$$

where  $|\mathbf{h}_s| = L$  and  $\nu$  is the number of delay taps of the channel.

Let  $\mathbf{H}_s$  denote an  $L \times L$  truncated Toeplitz matrix that has the channel vector  $\mathbf{h}_s$  as its first row. Then,  $\mathbf{H}_s$  is given by

$$\mathbf{H}_s = \begin{bmatrix} h_{s,1} & \dots & h_{s,d} & \dots & h_{s,\nu} & \dots & 0 \\ 0 & h_{s,1} & \dots & h_{s,d} & \dots & h_{s,\nu} & \dots 0 \\ \vdots & \ddots & \ddots & \ddots & \ddots & \ddots & \vdots \\ 0 & 0 & \dots & \dots & \dots & \dots 0 & \dots h_{s,1} \end{bmatrix} \quad (2)$$

Let  $\mathbf{x}$  and  $\hat{\mathbf{x}}_s$  be the transmission blocks with length  $L$  before and after CSD is applied, respectively, as depicted in Fig. 2.

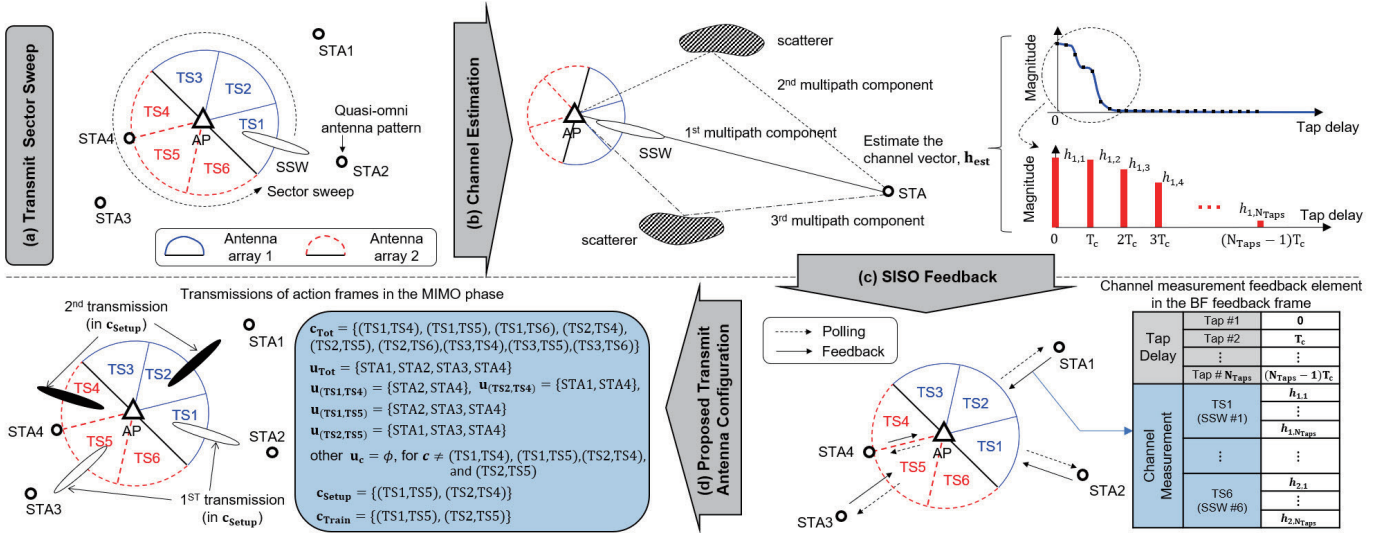


Fig. 3. Procedure of our proposed ILQE scheme: (a) transmit sector sweep, (b) channel estimation, (c) SISO feedback, and (d) transmit antenna configuration.

Using Eq. (2), when the  $N_t$  transmit antenna arrays are used simultaneously, the received signal can be defined as

$$\mathbf{y} = \sum_{s=1}^{N_t} (\sqrt{\rho} \cdot \mathbf{H}_s \cdot \hat{\mathbf{x}}_s) + \mathbf{n}, \quad (3)$$

where  $\rho$  is the transmit power and  $\mathbf{n}$  is zero-mean white Gaussian noise with covariance  $\sigma^2 \mathbf{I}_L$  [14].

Let  $\mathbf{H}_{cir}$  denote an  $L \times L$  truncated Toeplitz matrix of which the first row includes the channel vectors of all  $N_t$  antenna arrays and to which the CSD has been applied. Let  $\delta_s$  be a time shift for the CSD of the  $s^{\text{th}}$  antenna array; it is given by  $\delta_s = (s - 1) \cdot \delta_0$ , where  $\delta_0$  is a constant satisfying  $(\delta_0 \bmod T_c) = 0$  [2]. Then, the first row of  $\mathbf{H}_{cir}$  is given by

$$\mathbf{h}_{cir} = \sum_{s=1}^{N_t} S(\mathbf{h}_s, \delta_s), \quad (4)$$

where  $S(\cdot)$  cyclically shifts the vector  $\mathbf{h}_s$  to the right by  $\delta_s/T_c$ .

Thus, we can convert Eq. (3) as follows [13]:

$$\mathbf{y} = \sqrt{\rho} \cdot \mathbf{H}_{cir} \cdot \mathbf{x} + \mathbf{n}, \quad (5)$$

where  $\mathbf{x} = [x(L), \dots, x(1)]^T$ .

Given the channel matrix  $\mathbf{H}_{cir}$ , the minimum mean-square-error (MMSE) equalizer is

$$\mathbf{G} = \left( \varphi^{-1} \cdot \mathbf{I}_L + \mathbf{H}_{cir}^* \mathbf{H}_{cir} \right)^{-1} \mathbf{H}_{cir}^*, \quad (6)$$

where  $\varphi$  is the SNR and is given by  $\varphi = \frac{\rho}{\sigma^2}$ .

Using Eqs. (5) and (6), the equalized signal is

$$\hat{\mathbf{y}} = \sqrt{\rho} \cdot \mathbf{G} \mathbf{H}_{cir} \mathbf{x} + \mathbf{G} \mathbf{n}. \quad (7)$$

Let  $\mathbf{g}_k$  and  $\mathbf{h}_{cir}^{(k)}$  denote the  $k^{\text{th}}$  row of the matrix  $\mathbf{G}$  and the  $k^{\text{th}}$  column of the matrix  $\mathbf{H}_{cir}$ , respectively. Then, referring to Eq. (7), the signal to interference plus noise ratio (SINR) at the  $k^{\text{th}}$  value of the equalized signal  $\hat{\mathbf{y}}$  can be obtained as

follows [15]:

$$\gamma_k = \frac{\rho (\|\mathbf{g}_k \mathbf{h}_{cir}^{(k)}\|_2)^2}{\rho \sum_{l \neq k} (\|\mathbf{g}_k \mathbf{h}_{cir}^{(l)}\|_2)^2 + \sigma^2 \mathbf{g}_k \mathbf{g}_k^*} \quad (8)$$

Once the channel information is received from an STA during the SISO phase, the AP can obtain the channel vector  $\mathbf{h}_s$  of each antenna array  $s$  for a given candidate set of TSs. Then, using Eqs. (2)-(8), the AP estimates the link quality, i.e., the SINR measured at the STA at which the candidate sets of TSs are used. The following subsection describes how the AP receives the channel information from the STA and Subsection III-C presents how the SINR obtained from the equations in this subsection is used to determine an appropriate transmit antenna configuration.

### B. Channel Estimation and Feedback

In the transmit sector sweep of the SISO phase, an STA estimates the channel vector whenever the STA receives each short SSW frame. To this end, the legacy-channel estimation field (L-CEF) of the short SSW frame is used. The L-CEF includes a concatenation of two sequences  $\mathbf{G}\mathbf{u}_{512}$  and  $\mathbf{G}\mathbf{v}_{512}$  to leverage the auto-correlation property of a Golay complementary pair [2]. In practical wireless systems, the carrier frequency offset and time synchronization affect the accuracy of the channel estimation. This problem has been addressed in many prior studies [8], [16]. In this paper, we assume perfect time synchronization and negligible carrier frequency offset to estimate the channel vector.

The channel vector is estimated by correlating the received signal with the sequences,  $\mathbf{G}\mathbf{u}_{512}$  and  $\mathbf{G}\mathbf{v}_{512}$ . Let  $\mathbf{y}_{CEF}$  denote a set of symbols received for the L-CEF of length 1152. Then, the correlation with the first sequence,  $\mathbf{G}\mathbf{u}_{512}$ , is given by

$$\mathbf{h}_{Gu}[l] = \frac{1}{512} \sum_{k=1}^{512} \mathbf{y}_{CEF}[l+k-1] \cdot \mathbf{G}\mathbf{u}_{512}^*[k] \quad (9)$$

The correlation,  $\mathbf{h}_{Gv}[l]$ , with  $\mathbf{G}\mathbf{v}_{512}$  can be similarly expressed by substituting  $\mathbf{y}_{CEF}[l+k+511]$  and  $\mathbf{G}\mathbf{v}_{512}^*[k]$  for  $\mathbf{y}_{CEF}[l+k-1]$  and  $\mathbf{G}\mathbf{u}_{512}^*[k]$  in Eq. (9), respectively. Using these two correlations and referring to [17], the estimated channel vector can be obtained as follows:

$$\mathbf{h}_{est}[l] = \frac{\mathbf{h}_{Gu}[l] + \mathbf{h}_{Gv}[l]}{2}, \quad (10)$$

where  $l$  is an integer in the range  $[1, 128]$  to restrict the channel delay from spreading within the zero correlation zone of the Golay sequences in the L-CEF. The L-CEF field follows the sequence  $-Ga_{128}$  and ends with the sequence  $-Gb_{128}$ , facilitating the creation of a length-127 zero correlation zone after the peak [16].

Once the transmit sector sweep are completed, the STA sends the estimated channel information to the AP. As depicted in Fig. 1(a), each STA transmits a BRP frame during the SISO feedback subphase. The IEEE 802.11ay standard has defined a channel measurement feedback element that enables the BRP frame to contain the channel information [2]. Fig. 3(c) illustrates the implementation of the channel measurement feedback element. The channel vector,  $\mathbf{h}_{est}$ , represents the channel coefficients for 128 delay taps. Let  $N_{taps}$  be the number of taps for which the channel coefficients are included in the channel measurement feedback element; then, the STA determines the  $N_{taps}$  taps with larger magnitude in  $\mathbf{h}_{est}$ . The Tap Delay field of the channel measurement feedback element contains the delays of the  $N_{taps}$  taps in units of  $T_c$ . The Channel Measurement field contains the channel coefficients for the  $N_{taps}$  taps corresponding to each SSW frame.

### C. ILQE-Based Transmit Antenna Configuration

We explain our proposed ILQE scheme and present the simple example scenario in Fig. 3(d) for ease of comprehension.

**Candidate sets of TSs and their corresponding SINRs:** Our proposed ILQE scheme lists all candidate sets of TSs to be used to transmit action frames for MU-MIMO BFT. Let  $\mathbf{c}_{Tot}$  denote a collection of all candidate sets of TSs; then,  $\mathbf{c}_{Tot}$  consists of all combinations of TSs that are included in at least one of the SISO feedbacks received from STAs in the MU group. Let  $c \in \mathbf{c}_{Tot}$  be a candidate set of TSs; then, this set is given by  $c = (\alpha_1, \dots, \alpha_s, \dots, \alpha_{N_t})$ , where  $\alpha_s$  is a TS associated with the  $s^{\text{th}}$  antenna array.

Let  $\mathbf{u}_{Tot}$  be a set of STAs in the MU group. Our ILQE scheme estimates each SINR measured at each STA  $u \in \mathbf{u}_{Tot}$  when all TSs in each candidate set  $c \in \mathbf{c}_{Tot}$  are used simultaneously. Given the candidate set  $c = (\alpha_1, \dots, \alpha_s, \dots, \alpha_{N_t})$ , our scheme can obtain the channel vector  $\mathbf{h}_s$  in Eq. (1), which is associated with each TS  $\alpha_s$  ( $1 \leq s \leq N_t$ ); to this end, our scheme uses the channel information corresponding to the TS  $\alpha_s$ , which is included in the SISO feedback, i.e., the channel measurement feedback element, received from the STA  $u$ . If the channel measurement feedback element does not contain the channel information corresponding to the TS  $\alpha_s$ , the  $\mathbf{h}_s$  is a zero vector. Using channel vectors  $\mathbf{h}_s$  for all TSs  $\alpha_{vs}$  ( $1 \leq s \leq N_t$ ) and Eqs. (2)-(8), the average SINR

of an action frame with length  $L$  is estimated as follows:

$$\gamma_{avg}(u, c) = \frac{1}{L} \sum_{k=1}^L \gamma_k(u, c), \quad (11)$$

where  $\gamma_k(u, c)$  is the SINR of the  $k^{\text{th}}$  received symbol when the STA  $u$  receives the action frame transmitted with the candidate set  $c$ , and can be obtained from Eq. (8).

#### STA subgroup associated with each candidate set of TSs:

Our ILQE scheme lists each subgroup of STAs that, when all TSs of each candidate set are used simultaneously, are within the reach of the corresponding transmission in the MU group. Let  $\mathbf{u}_c$  be the subgroup of STAs that, given a candidate set  $c$ , are within the reach of the corresponding transmission in the MU group. Let  $\delta_{mu}$  be the minimum SINR that guarantees reliable transmission, i.e., the SINR threshold. Then, using Eq. (11), an STA  $u \in \mathbf{u}_{Tot}$  is included in the subgroup  $\mathbf{u}_c$  if its SINR estimated with candidate set  $c$  is greater than the SINR threshold, i.e.,  $\gamma_{avg}(u, c) \geq \delta_{mu}$ ; however, if its SINRs for all candidate sets are lower than the SINR threshold, i.e., if  $\gamma_{avg}(u, c) < \delta_{mu}$  for  $\forall c \in \mathbf{c}_{Tot}$ , the STA  $u$  is excluded from the MIMO phase. We define the remaining MU group as the subgroup of STAs in the MU group that are allowed to engage in the MIMO phase.

#### Transmit antenna configuration for the MIMO phase:

Our ILQE scheme determines appropriate sets of TSs, i.e., transmit antenna configurations, to transmit action frames for the MIMO phase. In the BF setup and selection subphases, the AP repeats the transmission of an action frame with a different set of TSs, such that all STAs in the remaining MU group can receive the action frame. To reduce signaling overhead, whenever each transmission occurs, our ILQE scheme determines the corresponding set of TSs with which the transmission reaches the largest number of STAs in the remaining MU group that have not received the action frame yet. Let  $\mathbf{c}_{Setup}$  be a collection of sets of TSs to be used for the transmissions of an action frame in the BF setup or selection subphase; then, Algorithm 1 presents the procedure for obtaining the collection  $\mathbf{c}_{Setup}$ .

In the NRC BF training subphase, the AP performs BFT with subgroups of STAs in the remaining MU group that are within reach of the transmission of BRP-RX/TX frames, respectively. Let  $\mathbf{c}_{Train}$  be a collection of sets of TSs to be used for the transmissions of BRP-RX/TX frames. Then, to mitigate signaling overhead, our ILQE scheme selects all sets of TSs in  $\mathbf{c}_{Tot}$ , to be included in  $\mathbf{c}_{Train}$ , satisfying that any two of the subgroups associated with the selected sets, e.g.,  $\mathbf{u}_c$  and  $\mathbf{u}_{c'}$ , are not a subset of each other, i.e.,  $\mathbf{u}_c \not\subset \mathbf{u}_{c'}$  and  $\mathbf{u}_{c'} \not\subset \mathbf{u}_c$ ; we assume that the AP can perform BFT with subsets of the subgroup  $\mathbf{u}_c$  using the same BRP-RX/TX frame transmitted through the TSs of the set  $c$  by choosing appropriate transmit AWVs for TRN subfields. Algorithm 2 presents the procedure for obtaining the collection  $\mathbf{c}_{Train}$ .

In the NRC BF feedback and the RC BF training subphases, for each STA in the remaining MU group, our ILQE scheme selects a set of TSs that is used to estimate the highest SINR at the STA. Let  $\mathbf{c}_{poll}^u$  be a set of TSs to be used when transmitting

---

**Algorithm 1** Transmit antenna configuration for the BF setup or selection subphase
 

---

```

1: Initialize  $\mathbf{c}_{\text{Setup}}$  to  $\phi$ ;  $\mathbf{u}_{\text{Tot}}$  includes all STAs in the remaining MU group;
2:  $\mathbf{c}_{\text{Tot}}$  includes all candidate sets of TSs.
3: while  $\mathbf{u}_{\text{Tot}} \neq \phi$  do // Repeat the process until  $\mathbf{u}_{\text{Tot}} = \phi$ .
4:    $c = \arg \max_{c' \in \mathbf{c}_{\text{Tot}}} |\mathbf{u}_{c'}|$  // Step 1: Select a set of TSs  $c$ , with which the transmission reaches the largest number of
5:   // STAs; to this end, our scheme determines a candidate set  $c' \in \mathbf{c}_{\text{Tot}}$  of which
6:   // the subgroup  $\mathbf{u}_{c'}$  includes the largest number of STAs.
7:    $\mathbf{c}_{\text{Setup}} \leftarrow c$ ; // Step 2: Include the selected set  $c$  in  $\mathbf{c}_{\text{Setup}}$ .
8:   for each  $c' \in \mathbf{c}_{\text{Tot}}$  do
9:     if  $\mathbf{u}_{c'} \subset \mathbf{u}_c$  then // Step 3: Remove all candidate sets  $c'$  from  $\mathbf{c}_{\text{Tot}}$  if the transmission corresponding to
10:    // the selected set  $c$  can reach all STAs in the subgroup associated with the
11:    // candidate set  $c'$ , i.e., if  $\mathbf{u}_{c'} \subset \mathbf{u}_c$ .
12:     $\mathbf{c}_{\text{Tot}} \leftarrow \mathbf{c}_{\text{Tot}} - \{c'\}$ ;
13:  // Step 4: Otherwise, if  $\mathbf{u}_{c'} \not\subset \mathbf{u}_c$ , STAs that are within reach of the transmission
14:  // corresponding to the selected set  $c$ , i.e.,  $u \in \mathbf{u}_c$ , are removed from
15:  // the subgroup associated with the candidate set  $c'$ , i.e.,  $\mathbf{u}_{c'} \leftarrow \mathbf{u}_{c'} - \{u\}$ .
16:  else
17:    for each  $u \in \mathbf{u}_c$  do
18:       $\mathbf{u}_{c'} \leftarrow \mathbf{u}_{c'} - \{u\}$ ;
19:    end for
20:  end if
21: end for
22: end while

```

---



---

**Algorithm 2** Transmit antenna configuration for the NRC BF training subphase
 

---

```

1: Initialize  $\mathbf{c}_{\text{Setup}}$  to  $\phi$ ;  $\mathbf{u}_{\text{Tot}}$  includes all STAs in the remain-
2: // ing MU group;
3:  $\mathbf{c}_{\text{Tot}}$  includes all candidate sets of TSs.
4: while  $\mathbf{c}_{\text{Tot}} \neq \phi$  do // Repeat the process until  $\mathbf{c}_{\text{Tot}} = \phi$ .
5:    $c = \arg \max_{c' \in \mathbf{c}_{\text{Tot}}} |\mathbf{u}_{c'}|$ 
6:   // Same as Step 1 of Algorithm 1
7:    $\mathbf{c}_{\text{Train}} \leftarrow c$ ; // Include the selected set  $c$  in  $\mathbf{c}_{\text{Train}}$ .
8:   for each  $c' \in \mathbf{c}_{\text{Tot}}$  do
9:     if  $\mathbf{u}_{c'} \subset \mathbf{u}_c$  then
10:    // Same as Step 3 of Algorithm 1
11:     $\mathbf{c}_{\text{Tot}} \leftarrow \mathbf{c}_{\text{Tot}} - \{c'\}$ ;
12:  end if
13: end for
14: end while

```

---

a BF poll frame to STA  $u$ ; then, using Eq. (11), it is given by

$$c_{\text{poll}}^u = \arg \max_{c \in \mathbf{c}_{\text{Tot}}} \gamma_{\text{avg}}(u, c) \quad (12)$$

**Example scenario in Fig. 3(d):** The AP has two antenna arrays, each of which is associated with three TSs; TSs 1 to 3 belong to antenna array 1 and TSs 4 to 6 belong to antenna array 2. Four STAs, STA1-STA4, are included in the MU group. We assume that all TSs are included in at least one of the SISO feedbacks received from STA1-STA4. Consequently, the collection  $\mathbf{c}_{\text{Tot}}$  comprises nine candidate sets of TSs.

When TS1 and TS5 are used simultaneously, i.e., the candidate set is (TS1, TS5), we assume that the corresponding transmission can reach STA2, STA3, and STA4; hence, the subgroup  $\mathbf{u}_{(\text{TS1}, \text{TS5})}$  includes these three STAs. Likewise, our scheme can obtain the subgroups,  $\mathbf{u}_{(\text{TS1}, \text{TS4})}$ ,  $\mathbf{u}_{(\text{TS2}, \text{TS4})}$ , and

$\mathbf{u}_{(\text{TS2}, \text{TS5})}$ , and we assume that the transmissions corresponding to all candidate sets other than (TS1, TS5), (TS1, TS4), (TS2, TS4), and (TS2, TS5) do not reach the STAs.

The collection  $\mathbf{c}_{\text{Setup}}$  includes the sets of TSs (TS1, TS5) and (TS2, TS4). This is because the transmission corresponding to the set (TS1, TS5) can reach the largest number of STAs, STA2, STA3, and STA4, i.e.,  $|\mathbf{u}_{(\text{TS1}, \text{TS5})}| = 3$ , and the transmission corresponding to the set (TS2, TS4) can reach STA1, which did not receive the previous transmission.

The collection  $\mathbf{c}_{\text{Train}}$  includes the sets of TSs (TS1, TS5) and (TS2, TS5), but excludes the sets of TSs (TS1, TS4) and (TS2, TS4) because their subgroups  $\mathbf{u}_{(\text{TS1}, \text{TS4})}$  and  $\mathbf{u}_{(\text{TS2}, \text{TS4})}$  are subsets of the subgroups  $\mathbf{u}_{(\text{TS1}, \text{TS5})}$  and  $\mathbf{u}_{(\text{TS2}, \text{TS5})}$ , respectively.

#### D. Heuristic Method for Lower Computational Complexity

The computational complexity of our ILQE scheme mainly depends on the estimation of SINRs measured at STAs when the candidate sets of TSs are used. To reduce the complexity, our scheme approximates the SINRs without the use of the matrix inversion and multiplication shown in Eqs. (6)-(8). Let  $\mathbf{H}_{\text{toe}}$  denote an  $L \times L$  Toeplitz matrix whose first row is  $\mathbf{h}_{\text{cir}}$  obtained from Eq. (4). Our scheme then uses  $\mathbf{H}_{\text{toe}}$  in Eq. (5), instead of using the truncated Toeplitz matrix  $\mathbf{H}_{\text{cir}}$ ; it has little effect on the average SINR obtained from Eq. (11) because the number of symbols  $L$  is much greater than the number of delay taps  $\nu$  in Eq. (1), i.e.,  $L \gg \nu$ . Referring to [13], when  $\mathbf{H}_{\text{toe}}$  is used and the MMSE equalizer is considered, the average SINR measured at STA  $u$  when a set  $c \in \mathbf{c}_{\text{Tot}}$  is used can be approximated as follows:

$$\gamma_{\text{toe}}^{\text{MMSE}}(u, c) = \left[ \frac{1}{L} \cdot \sum_{k=1}^L \frac{1}{1 + \varphi \cdot (\|\lambda_k\|_2)^2} \right]^{-1} - 1 \quad (13)$$

where  $\{\lambda_k\}_{k=1}^L$  are the eigenvalues of  $\mathbf{H}_{toe}$  and given  $\mathbf{h}^{cir} = [h_1^{cir}, \dots, h_{l'}^{cir}, 0, \dots, 0]$ , it is computed as  $\lambda_k = \sum_{l=1}^{l'} h_l^{cir} e^{-j \frac{2\pi(l-1)(k-1)}{L}}$ .

Our ILQE scheme also uses a heuristic method to significantly reduce the number of times the SINRs are computed. We assumed that owing to the transmit diversity gain, the SINR of multiple concurrent beams is greater than that of each single beam but less than the sum of those of all single beams. Under this assumption, our heuristic method selects the transmit antenna configuration for action frames transmitted in the MU-MIMO BFT by employing the SINRs of the single beams included in the SISO feedback. It then estimates the SINRs measured at STAs when the selected transmit antenna configuration is used to determine whether the selected transmit antenna configuration is appropriate. The detailed operations are as follows:

- 1) Let  $\Gamma$  denote the lookup table that contains each SINR measured at each STA  $u \in \mathbf{u}_{\text{Tot}}$  when all TSs in each candidate set  $c \in \mathbf{c}_{\text{Tot}}$  are used simultaneously. Initially,  $\Gamma(u, c)$  is simply set to the sum of the SINRs corresponding to all TSs in the candidate set  $c$  that have been known from the SISO feedback of the STA  $u$ ; if some TSs have not been known from the SISO feedback, their SINRs are considered to be zero.
- 2) Obtain each STA subgroup  $\mathbf{u}_c$  associated with each candidate set  $c \in \mathbf{c}_{\text{Tot}}$  and determine the transmit antenna configurations  $\mathbf{c}_{\text{Setup}}$ ,  $\mathbf{c}_{\text{Train}}$ , and  $\mathbf{c}_{\text{Poll}}^u$  in the same manner as described in Section III-C by using  $\Gamma(u, c)$  instead of  $\gamma_{\text{avg}}(u, c)$  in Eq. (11).
- 3) Update  $\Gamma(u, c)$  to  $\gamma_{toe}^{MMSE}(u, c)$  in Eq. (13) for  $\forall u \in \mathbf{u}_c$  and  $\forall c \in \mathbf{c}_{\text{Setup}}$ , if  $\Gamma(u, c)$  has never been updated and if the SINRs corresponding to the TSs in the set  $c$ , which have been known from the SISO feedback of STA  $u$ , are all less than the SINR threshold  $\delta_{mu}$  plus a predetermined margin value.
- 4) Perform step 3 again for  $\mathbf{c}_{\text{Train}}$  and  $\mathbf{c}_{\text{Poll}}^u$ , respectively, in place of  $\mathbf{c}_{\text{Setup}}$ .
- 5) Repeat steps 2 to 4 until there are no updates in the lookup table  $\Gamma$ .

#### IV. PERFORMANCE ANALYSIS

In this section, we analyze the BFT time of the NRC and RC MIMO phases considering the duration of each action frame transmitted in the control mode.

##### A. BFT Time of NRC MIMO Phase

An action frame comprises legacy-short training field (L-STF), L-CEF, L-Header, enhanced directional multi-enhanced directional multi-gigabit beam refinement protocol (EDMG)-Header-A, and TRN fields in addition to its payload field [2]. Let  $d_{\text{pre}}$  and  $d_{\text{trn}}$  denote the duration of the L-STF and L-CEF fields and the duration of the TRN field, respectively. Let  $d_{\text{hp}}(\cdot)$  be the duration of the header and payload fields, given the length of the payload field. Then, the durations  $d_{\text{pre}}$ ,  $d_{\text{trn}}$ , and  $d_{\text{hp}}(\cdot)$  have been analyzed in our previous work [4].

In the MIMO phase, each subphase is separated by medium beamforming interframe space (MBIFS), and each transmission in a subphase is separated by short interframe space (SIFS), as depicted in Figs. 1(b) and (c). The duration of a BF setup frame is

$$d_{\text{setup}} = d_{\text{pre}} + d_{\text{hp}}(l_{\text{setup}}), \quad (14)$$

where  $l_{\text{setup}}$  is the length of the payload field of the BF setup frame. Similarly, the duration of a BRP-RX/TX frame with the TRN field is

$$d_{\text{train}} = d_{\text{pre}} + d_{\text{hp}}(l_{\text{train}}) + d_{\text{trn}}, \quad (15)$$

where  $l_{\text{train}}$  is the length of the payload field of the BRP-RX/TX frame.

Let  $d_{\text{SIFS}}$  be the duration of an SIFS. Then, using Eq. (14), the duration of the BF setup subphase is

$$D_{\text{Setup}} = |\mathbf{c}_{\text{Setup}}| \cdot d_{\text{setup}} + (|\mathbf{c}_{\text{Setup}}| - 1) \cdot d_{\text{SIFS}}. \quad (16)$$

The duration of the BF training subphase, denoted by  $D_{\text{Train}}$ , can be obtained by substituting  $\mathbf{c}_{\text{Train}}$  and  $d_{\text{train}}$  for  $\mathbf{c}_{\text{Setup}}$  and  $d_{\text{setup}}$  in Eq. (16), respectively.

In the BF feedback subphase, the AP sends a BF poll frame to each STA. Let  $l_{\text{poll}}$  be the length of the payload field of the BF poll frame. Then, the duration of the BF poll frame, denoted by  $d_{\text{poll}}$ , can be obtained by substituting  $l_{\text{poll}}$  for  $l_{\text{setup}}$  in Eq. (14). If an STA  $u$  fails to receive the corresponding BF poll frame, the AP waits for a time period, denoted by  $d_{\text{wait}}$ , and then polls another STA in the remaining MU group. Let  $P_e(\cdot)$  denote the function to obtain bit error rate for the transmission of an action frame; the input to this function is the average SINR of the transmission, which can be calculated from Eq. (11). We represent the function  $P_e(\cdot)$  as an offline lookup table that maps each SINR to the corresponding bit error rate [18]. Then, the probability that the STA  $u$  fails to receive the BF poll frame because of an error is

$$P_{\text{poll}}^{\text{fail}}(u) = 1 - \{1 - P_e(\gamma_{\text{avg}}(u, \mathbf{c}_{\text{Poll}}^u))\}^{l_{\text{poll}}}. \quad (17)$$

If the STA  $u$  successfully receives the BF poll frame, the STA  $u$  sends a BF feedback frame to the AP; however, the STA  $u$  cannot send the frame in the following two situations (**Condition 1**):

- Case 1: The STA  $u$  fails to receive the BF setup frame in the BF setup subphase.
- Case 2: The STA  $u$  successfully receives the BF setup frame, but fails to receive any BRP-RX/TX frame in the BF training subphase.

The probability of Case 1 above is

$$P_{\text{case1}}^{\text{fail}}(u) = \prod_{c \in \mathbf{c}_{\text{Setup}}} \left[ 1 - \{1 - P_e(\gamma_{\text{avg}}(u, c))\}^{l_{\text{setup}}} \right]. \quad (18)$$

Let  $P_{\text{train}}^{\text{fail}}(u)$  be the probability that the STA  $u$  fails to receive any BRP-RX/TX frame in the BF training subphase; the probability is given by substituting  $\mathbf{c}_{\text{Train}}$  and  $l_{\text{train}}$  for  $\mathbf{c}_{\text{Setup}}$  and  $l_{\text{setup}}$ , respectively, in Eq. (18). Then, the probability of

Case 2 is

$$P_{\text{case2}}^{\text{fail}}(u) = \{1 - P_{\text{case1}}^{\text{fail}}(u)\} \cdot P_{\text{train}}^{\text{fail}}(u). \quad (19)$$

Let  $l_{\text{feed}}$  be the length of the payload field of the BF feedback frame. As described in Section II-A, the BF feedback frame includes multiple measurements of the link quality and information regarding the corresponding transmit and receive antennas. Let  $n_{\text{meas}}$  be the number of the link-quality measurements included. Then, referring to [2], the  $l_{\text{feed}}$  is given by

$$l_{\text{feed}} = 47 + \lceil n_{\text{meas}} \cdot 31/8 \rceil. \quad (20)$$

The duration of the BF feedback frame, denoted by  $d_{\text{feed}}$ , can be obtained by substituting  $l_{\text{feed}}$  for  $l_{\text{setup}}$  in Eq. (14).

If an STA corresponds to Case 1 or Case 2 of **Condition 1**, we assume that the STA does not send the BF feedback frame and the AP has to wait for a time period  $d_{\text{wait}}$ ; otherwise, for ease of exposition, we assume that the AP receives the BF feedback frames from the STA without error. Thus, using Eqs. (17)-(20), the duration of the BF feedback subphase is

$$D_{\text{Feed}} = \sum_{u \in \mathbf{u}_{\text{Tot}}} \left[ d_{\text{poll}} + P_{\text{poll}}^{\text{fail}}(u) \cdot d_{\text{wait}} + (1 - P_{\text{poll}}^{\text{fail}}(u)) \cdot \{P_{\text{feed}}^{\text{fail}}(u) \cdot d_{\text{wait}} + (1 - P_{\text{feed}}^{\text{fail}}(u)) \cdot (d_{\text{feed}} + 2d_{\text{SIFS}})\} \right], \quad (21)$$

where  $P_{\text{feed}}^{\text{fail}}(u) = P_{\text{case1}}^{\text{fail}}(u) + P_{\text{case2}}^{\text{fail}}(u)$ .

After the BF feedback subphase is completed, if all the STAs correspond to Case 1 or Case 2 in **Condition 1** or if all STAs fail to receive the corresponding BF poll frames, the AP does not perform the BF selection subphase; the probability of which is

$$P_{\text{selec}}^{\text{fail}} = \prod_{u \in \mathbf{u}_{\text{Tot}}} \left[ P_{\text{case1}}^{\text{fail}}(u) + P_{\text{case2}}^{\text{fail}}(u) + \{1 - P_{\text{case1}}^{\text{fail}}(u)\} \cdot \{1 - P_{\text{train}}^{\text{fail}}(u)\} \cdot P_{\text{poll}}^{\text{fail}}(u) \right]. \quad (22)$$

Let  $l_{\text{selec}}$  be the length of the payload field of the BF selection frame. This selection frame includes information regarding the configuration of the receive antenna for the transmit AWWs selected for DL MU-MIMO transmission through the BF training subphase. Let  $n_{\text{config}}$  be the number of selected transmit AWWs; then, let  $n_{\text{sta}}$  be the average number of STAs associated with each transmit antenna array for each selected transmit AWW. Referring to [2], the  $l_{\text{selec}}$  is

$$l_{\text{selec}} = 33 + \lceil 40 + n_{\text{config}} \cdot N_t \cdot (32 + 16 \cdot n_{\text{sta}})/8 \rceil. \quad (23)$$

The duration of the BF selection frame, denoted by  $d_{\text{selec}}$ , can be obtained by substituting  $l_{\text{selec}}$  for  $l_{\text{setup}}$  in Eq. (14), and the duration of the BF selection subphase, denoted by  $D_{\text{Selec}}$ , can be obtained by substituting  $d_{\text{selec}}$  for  $d_{\text{setup}}$  in Eq. (16).

Thus, using Eqs. (16) and (21)-(23), the nanosecond duration of the NRC MIMO phase is

$$D_{\text{NRC}} = D_{\text{Setup}} + D_{\text{Train}} + D_{\text{Feed}} + (1 - P_{\text{selec}}^{\text{fail}}) \cdot (d_{\text{MBIFS}} + D_{\text{Selec}}) + 2d_{\text{MBIFS}}, \quad (24)$$

where  $d_{\text{MBIFS}}$  is the duration of MBIFS.

## B. BFT Time of RC MIMO Phase

The BF setup and selection subphases of the RC MIMO phase are the same as those of the NRC MIMO phase. However, the BF training subphase of the RC MIMO phase operates in the same manner as the BF feedback subphase of the NRC MIMO phase, as depicted in Fig. 1(c); the AP polls each STA, which sends back the BRP-RX/TX frame to the AP. Let  $D_{\text{Train}}^{\text{RC}}$  be the duration of the BF training subphase. Then, the duration  $D_{\text{Train}}^{\text{RC}}$  can be obtained by substituting  $d_{\text{train}}$  and  $P_{\text{case1}}^{\text{fail}}(u)$  for  $d_{\text{feed}}$  and  $P_{\text{feed}}^{\text{fail}}(u)$ , respectively, in Eq. (21).

After the BF training subphase is completed, if all the STAs correspond to Case 1 in **Condition 1** or if all the STAs fail to receive all the corresponding BF poll frames, the AP does not perform the BF selection subphase; thus, referring to Eq. (22), its probability is

$$P_{\text{selec}}^{\text{RC}} = \prod_{u \in \mathbf{u}_{\text{Tot}}} \left[ P_{\text{case1}}^{\text{fail}}(u) + \{1 - P_{\text{case1}}^{\text{fail}}(u)\} \cdot P_{\text{poll}}^{\text{fail}}(u) \right]. \quad (25)$$

Referring to Eq. (24) and Fig. 1(c), the nanosecond duration of the RC MIMO phase is

$$D_{\text{RC}} = D_{\text{Setup}} + D_{\text{Train}}^{\text{RC}} + (1 - P_{\text{selec}}^{\text{RC}}) \cdot (d_{\text{MBIFS}} + D_{\text{Selec}}) + d_{\text{MBIFS}}. \quad (26)$$

## V. SIMULATION: RESULTS AND DISCUSSION

We implemented simulation programs with ns-3 and MATLAB, as depicted in Fig. 4, and then evaluated our ILQE scheme by comparing it with the existing LSB and LNS schemes.

**Q-D Channel Model:** For the evaluation, we used the Q-D channel model that was adopted by the IEEE 802.11ay task group to accurately represent the signal propagation [19]. This approach enables the mmWave channel between the transmitter and the receiver to be characterized by the direct and specular multipath components. The properties of each multipath component, i.e., pathloss, delay, phase shift, angle of arrival, and angle of departure, are ray-traced for a given deployment [20].

We assume that every antenna array comprises  $N$  elements. A steering vector represents the set of phase delays that a plane wave experiences as it reaches each element in an antenna array. For wave propagation in a direction described by the elevation angle  $\theta$  and azimuth angle  $\phi$ , the wave vector  $\mathbf{k}$  is given by

$$\mathbf{k} = \frac{2\pi}{\beta} (\sin \theta \cos \phi, \sin \theta \sin \phi, \cos \theta), \quad (27)$$

where  $\beta$  denotes the wavelength of the signal. This enables us to obtain the steering vector representing the relative phases at an antenna array as follows:

$$\mathbf{a}(\phi, \theta) = [e^{-j\mathbf{k}r_1}, e^{-j\mathbf{k}r_2}, \dots, e^{-j\mathbf{k}r_i}, \dots, e^{-j\mathbf{k}r_N}]^T, \quad (28)$$

where  $r_i$  is the point of the  $i^{\text{th}}$  element with the coordinates  $(x_i, y_i, z_i)$ .

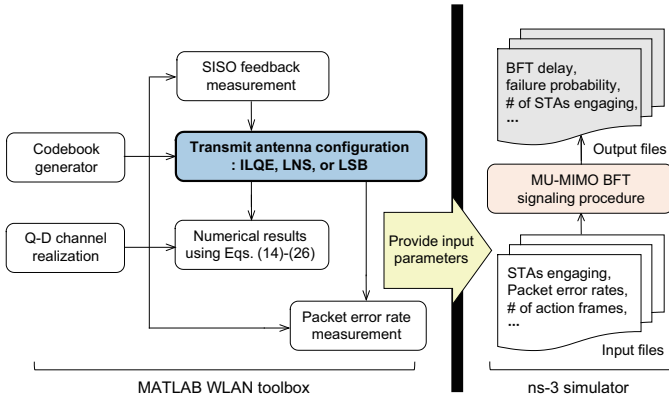


Fig. 4. Implementation of numerical method and simulation with ns-3 and MATLAB.

Let  $M$  and  $f$  be the total number of multipath components and the operating frequency of the system, respectively. Let  $\mathbf{w}_t$  and  $\mathbf{w}_r$  denote the weight vectors used in the antenna arrays of the transmitter and receiver, respectively, satisfying  $\|\mathbf{w}_r[i]\|_2 = \|\mathbf{w}_t[i]\|_2 = \sqrt{N^{-1}}$ . Then, referring to [19], we can define the channel impulse response of the beamformed channel between the  $s^{\text{th}}$  transmit and receive antenna arrays, as follows:

$$h_s^{BF}(t) = \frac{1}{\sqrt{M}} \sum_{m=1}^M \left( \alpha_m \cdot e^{j2\pi f t_m} \cdot \delta(t - t_m) \cdot \mathbf{w}_r \cdot \mathbf{a}_r(\phi_m^a, \theta_m^a) \cdot \mathbf{a}_t(\phi_m^d, \theta_m^d)^* \cdot \mathbf{w}_t \right), \quad (29)$$

where  $\phi_m^a$  ( $\theta_m^a$ ) and  $\phi_m^d$  ( $\theta_m^d$ ) are the azimuth (elevation) angles of arrival and departure, respectively, and  $t_m$  is the arrival delay for the  $m^{\text{th}}$  multipath component;  $\delta(\cdot)$  is the Dirac delta function;  $\mathbf{a}_t(\cdot)$  and  $\mathbf{a}_r(\cdot)$  are the steering vectors of the transmit and receive antenna arrays, respectively, and can be obtained from Eq. (28). In Eq. (29),  $\alpha_m$  is the complex amplitude and is given by [11]

$$\alpha_m = 10^{-PL_m/20} \cdot e^{j \cdot phase_m}, \quad (30)$$

where  $PL_m$  and  $phase_m$  are the path loss and phase shift, respectively, of the  $m^{\text{th}}$  multipath component.

The channel impulse response of the beamformed channel,  $h_s^{BF}(t)$ , is used to obtain the channel vector,  $\mathbf{h}_s$ , in Eq. (1), which employs an equivalent uniformly spaced tapped delay line [21]. Then, we use Eqs. (2)-(8) to calculate the SINR of each action frame transmitted in the MIMO phase.

**System and environmental parameters:** The propagation environment is a cuboid of size  $(10 \times 19 \times 3)$  m [19]. An MU group included one AP and eleven STAs; the AP was located at the coordinates  $(1, 3, 1)$  m and the STAs were randomly distributed, as depicted in Fig. 5(a). We used Q-D channel realization software to model the specular nature of the mmWave reflections using the method of geometrical optics [22]. The maximum number of multipath components between the AP and each STA was seven, one line-of-sight path, and six first-

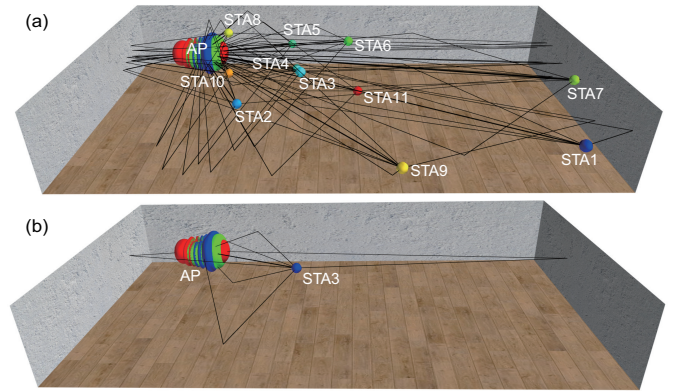


Fig. 5. (a) Examples of simulation scenarios and (b) seven multipath components (black lines in the figure) between AP and STA3.

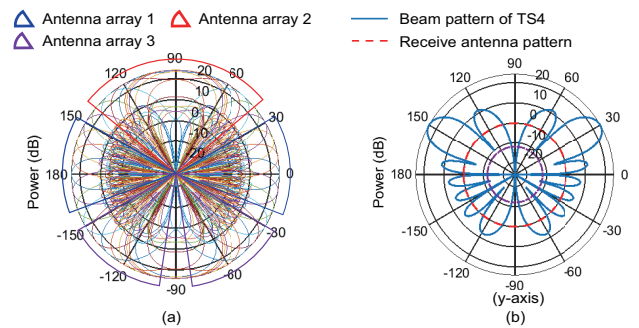


Fig. 6. (a) Azimuth-cut patterns of all TSs when each antenna array is associated with six azimuth angles,  $\phi_t$ , and (b) beam pattern of TS 4 ( $\phi_t = 30^\circ$  or  $150^\circ$ ) and the receive antenna pattern.

order specular reflections, as depicted in Fig. 5(b). Specifically, the Q-D channel realization software generated the following channel properties of each multipath component: delay, path gain, phase offset, angle of arrival, and angle of departure. The path loss of the  $m^{\text{th}}$  multipath component was given by  $PL_m = 20 \log_{10}(4\pi d_m / \beta)$ , where  $d_m$  is the length of the multipath component; its phase shift,  $phase_m$ , was considered to be  $\pi$  for the first-order reflection [11].

The AP utilized a uniform planar array in which the array elements lie on the  $yz$ -plane [14]; the inter-element spacing was  $\beta/2$  and  $N = 16$  (i.e.,  $2 \times 8$ ). Using Codebook Generator in [22], we generated the steering vector of Eq. (28) and divided the azimuth plane into multiple TSs. The AWV of each TS was defined as follows. Let  $\phi_t$  and  $\theta_t$  be the azimuth and elevation angles, respectively, of a TS; then, its transmit AWV is given by  $\mathbf{w}_t = \sqrt{N^{-1}} \cdot \mathbf{a}_t(\phi_t, \theta_t)$ , where  $\theta_t$  was fixed to  $\pi/2$ . The azimuth angles,  $\phi_t$ , were uniformly distributed with an interval of  $\pi/18$ . However, in MATLAB, the beam pattern of each TS was symmetric about the plane of the array, i.e., the  $yz$ -plane, as depicted in Fig. 6(b); hence, we defined 18 TSs covering the entire range of azimuth angles,  $[0, 2\pi]$ , as depicted in Fig. 6(a). The total number of transmit antenna arrays,  $N_t$ , was set to 3 and each antenna array was associated with six different TSs. The STAs also utilized the uniform planar array but activated only the first array element to realize a quasi-omni pattern, as depicted in Fig. 6(b). Other parameters were

TABLE II  
PARAMETERS USED IN PERFORMANCE EVALUATION

Para.	Value	Para.	Value	Para.	Value	Para. ( $\mu s$ )	Value
$f$	60 GHz	$\beta$	4.96 mm	$N_t$	3	$d_{\text{feed}}$	43.7
$T_c$	0.57 ns	$\delta_0$	$4 \cdot T_c$	$N$	16	$d_{\text{trn}}$	146.21
$\rho$	10 or 2.5 dBm	$l_{\text{setup}}$	45	$d_{\text{SIFS}}$	$3 \mu s$	$d_{\text{pre}}$	4.3
$l_{\text{train}}$	55	$l_{\text{poll}}$	40	$d_{\text{MBIFS}}$	$9 \mu s$	$d_{\text{hp}}(l_{\text{setup}})$	20.87
$\sigma^2$	-90 or -85 dBm	$l_{\text{feed}}$	109	$d_{\text{setup}}$	$25.17 \mu s$	$d_{\text{hp}}(l_{\text{train}})$	22.33
$n_{\text{config}}$	8	$n_{\text{meas}}$	16	$d_{\text{train}}$	$172.84 \mu s$	$d_{\text{hp}}(l_{\text{poll}})$	20.14
$n_{\text{sta}}$	$\lfloor  \mathbf{u}_{\text{Tot}} /N_t \rfloor$	$M$	7	$d_{\text{poll}}$	$24.44 \mu s$	$d_{\text{hp}}(l_{\text{feed}})$	39.4

defined as presented in Table II [2],[4].

**IEEE 802.11ay transceiver:** Our numerical and simulation programs were derived from the 802.11ad implementation in the MATLAB WLAN toolbox; however, this implementation was modified to incorporate the Q-D channel model [20]. As depicted in Fig. 2, the bit stream of an action frame was scrambled to break up long bit sequences of contiguous 0's or 1's. The scrambled bit sequence was encoded using an effective low-density parity check (LDPC) code rate less than or equal to 1/2 to perform forward error correction. The coded bits were then converted into a stream of complex constellation points using differential binary phase shift keying. The constellation points were spread using a 32-length Golay sequence. The Q-D channel was realized using the Q-D channel realization software; this channel was applied with additive white Gaussian noise to the symbols, in the same manner as described in Section III-A. At the receiver, the operations of the transmitter were reversed to recover the transmitted bit.

**SISO feedback and transmit antenna configuration:** Once the SISO feedback was received, as described in Section III-B, the AP executed our proposed ILQE scheme in the same manner as presented in Section III-C. Specifically, in our simulation, the AP determined the STAs that engaged in the MIMO phase, number of action frames that were transmitted in each subphase, and antenna configurations that were used to transmit these action frames.

**Packet error rate:** Our simulation program using MATLAB measured the packet error rate of each action frame that was transmitted using the corresponding set of TSs. To this end, the AP sent the action frame to each STA a hundred times to enable the STA to compute its packet error rate. The packet error rates of all action frames that were measured by each STA, were used as input parameters to operate the signaling procedure of the MU-MIMO BFT implemented with ns-3.

**MU-MIMO BFT signaling:** We extended the open source code of [11] to implement the MU-MIMO BFT in ns-3. Our ns-3 simulation program employed the input files obtained from our MATLAB one, as depicted in Fig. 4. The input files enabled the AP to use the transmit antenna configuration determined by the proposed ILQE scheme; additionally, they enabled each STA to set the packet error rate of each action frame. The AP performed the MU-MIMO BFT at every beacon interval of 102.4 ms. A single ns-3 simulation trial had a running time of 90 s; in total, 879 BFTs were performed

per simulation trial. We ran hundreds of simulation trials by randomly distributing the positions of the STAs.

**Two comparison schemes:** The performance of our proposed ILQE scheme was compared with those of the existing schemes, LSB and LNS, presented in Section II-B. To evaluate these schemes, we utilized the same numerical and simulation programs as those used for our ILQE scheme; we only varied the operation of the transmit antenna configuration according to each existing scheme, as depicted in Fig. 4.

#### A. Performance of the NRC MIMO Phase

We considered two evaluation scenarios in which the AP used high and low transmit powers, respectively. In the case of the high transmit power, i.e.,  $\rho = 10$  dBm and  $\sigma^2 = -90$  dBm, all STAs were allowed to engage in the MIMO phase below the SINR threshold,  $\delta_{mu}$ , in the range of [1, 5] (ratio). However, in the other case, i.e., for low transmit power  $\rho = 2.5$  dBm and  $\sigma^2 = -85$  dBm, certain STAs were excluded from the MIMO phase because the transmissions corresponding to all candidate sets of TSs could not reach any of the STAs, i.e., the SINRs of these transmissions were estimated to be lower than the threshold  $\delta_{mu}$ . The error bars of Figs. 7 to 12 represent 99 % confidence intervals.

We first present the numerical and simulation results obtained for the high transmit power. Figs. 7(a)–(d) plot the duration of each subphase in the NRC MIMO phase. We found that, in the BF setup and selection subphases, i.e., Figs. 7(a) and (d), the duration of the running times of both the ILQE and LNS schemes increased as the threshold  $\delta_{mu}$  increased. This is because, as the threshold  $\delta_{mu}$  increased, each transmission of the AP was able to reach fewer STAs at a time, leading to the transmission of additional action frames. Figs. 7(a) and (d) also demonstrate that the duration of our scheme was shorter than that of the LNS scheme. This is because our ILQE scheme can identify a larger number of STAs than those within the reach of its transmission of an action frame, in comparison with the LNS scheme; hence, our scheme performed fewer transmissions to reach all the STAs.

Fig. 7(b) depicts a plot of the duration of the BF training subphase as a function of the SINR threshold. To compare the duration of our ILQE scheme with that of the LNS scheme, we assumed the following two situations:

- all available subgroups (AAS): Our ILQE scheme performed the MU-MIMO BFT with all subgroups of the

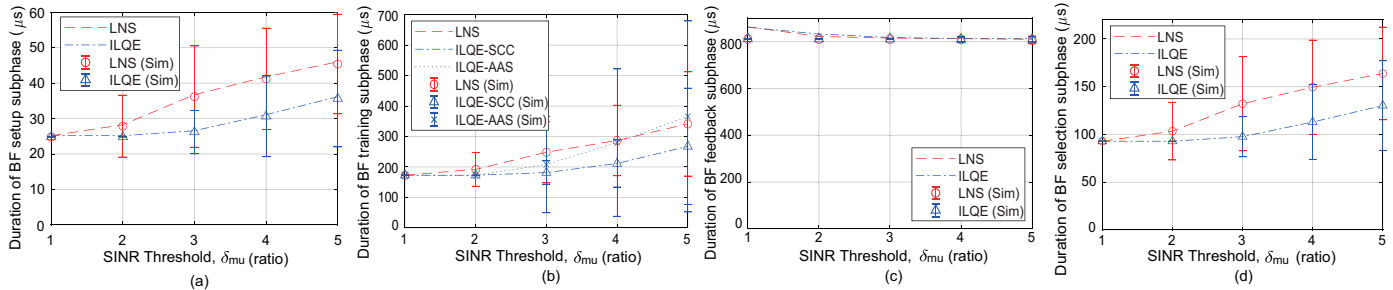


Fig. 7. Duration of (a) BF setup, (b) BF training, (c) BF feedback, and (d) BF selection subphases in the NRC MIMO phase for high transmit power, i.e.,  $\rho = 10$  dBm and  $\sigma^2 = -90$  dBm.

TABLE III  
PERFORMANCE OF THE LSB SCHEME BY SETTING THE SINR THRESHOLD TO 3 ( $\delta_{mu} = 3$ ).

Results	Duration of each NRC subphase ( $\mu s$ )				Duration of NRC MIMO phase ( $\mu s$ )	Duration of RC BF training subphase ( $\mu s$ )	Duration of RC MIMO phase ( $\mu s$ )
	BF setup	BF training	BF feedback	BF selection			
Numerical	120.4	1984	812.7	416.9	3361	2233.5	2788.9
Simulation	119	1982.9	810.6	416.9	3356.4	2231.5	2785.4

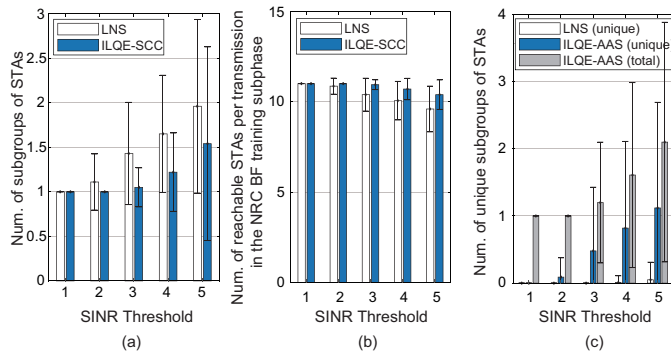


Fig. 8. NRC MIMO phase: (a) number of subgroups of STAs in the MU group within reach of transmissions, (b) number of STAs within reach of the transmission, and (c) number of unique subgroups of STAs determined by the LNS and ILQE schemes, respectively.

STAs in the MU group that could be reached by the BRP-RX/TX frames transmitted in the BF training subphase.

- same conditions as comparison schemes (SCC): Our scheme only supported the subgroups of STAs in the MU group that could be tested by the LNS and LSB schemes for the MU-MIMO BFT.

The results in Fig. 7(b) demonstrate that the duration time of our ILQE scheme was shorter than that of the LNS scheme to support the same subgroups, i.e., in the SCC case. This can be attributed to the fact that our scheme identified a greater number of reachable STAs for each transmission, i.e., the subgroup for each transmission included more STAs, and hence, our scheme transmitted fewer BRP-RX/TX frames, as depicted in Figs. 8(a) and (b).

Fig. 8(a) depicts the number of subgroups of STAs that were reached by the BRP-RX/TX frames transmitted by our ILQE scheme in the MU group; it indicates the number of transmissions during the BF training subphase, i.e.,  $|\mathbf{c}_{\text{Train}}|$ .

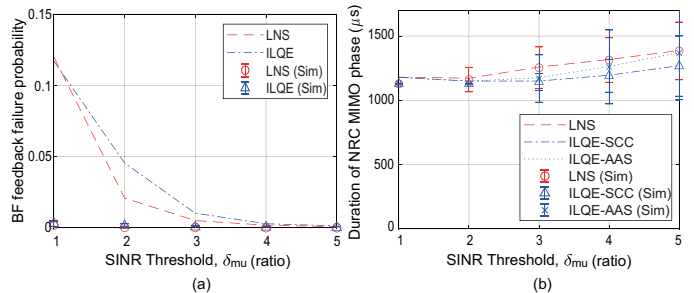


Fig. 9. (a) Probability that an STA cannot send the BF feedback frame and (b) total duration of the NRC MIMO phase when  $\rho = 10$  dBm and  $\sigma^2 = -90$  dBm.

For evaluation purposes, we define unique subgroups of ILQE and LNS as subgroups of ILQE and LNS that are not subsets of any subgroups of LNS and ILQE, respectively. Fig. 8(c) depicts that the subgroups of our ILQE scheme were able to include almost all subgroups of the LNS scheme; additionally, our ILQE scheme supported many different subgroups that the LNS scheme was unable to test.

The duration of the BF feedback subphase mainly depends on the number of STAs engaging in the MIMO phase. With high transmit power, all STAs were allowed to engage in both the ILQE and LNS schemes. Thus, Fig. 7(c) depicts that the results of both schemes were close to each other. Fig. 9(a) illustrates the probability of an STA not being able to send the BF feedback frame because of the reasons specified in **Condition 1**. The failure probabilities  $P_{\text{feed}}^{\text{fail}}(\cdot)$  were numerically calculated by using Eqs. (18) and (19). To obtain the function  $P_e(\cdot)$  in Eq. (18), we measured the bit error rates that correspond to SINRs in the range of  $[0.1, 10]$ , as depicted in Fig. 10. For these measurements, we employed the IEEE 802.11ay transceiver except for the Q-D channel model. The transmitter generated 5000 packets per SINR. The

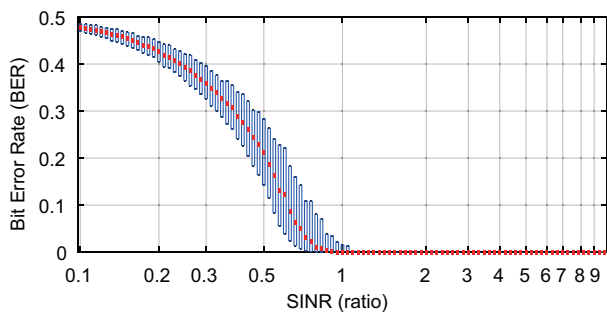


Fig. 10. bit error rate versus SINR in Control Mode (Box indicates the lower, median, and upper quartiles).

size of each packet was fixed at 1023 bytes and the SINR was adjusted with the additive white Gaussian noise channel.

Fig. 9(a) depicts that the behaviors of the numerical and simulation curves are similar although their values differ considerably. This difference results from the fact that the numerical failure probabilities were calculated from the bit error rate function  $P_e(\cdot)$ , which ignores the effect of the Q-D channel model. However, we found this difference to have little effect on the duration of the BF feedback subphase, as depicted in Fig. 7(c). Additionally, our results, particularly the simulation results, demonstrated that the failure probabilities of our scheme were close to those of the LNS scheme. Finally, the total duration of the NRC MIMO phase is plotted in Fig. 9(b).

The results of the LSB scheme remained almost constant regardless of the value of the threshold  $\delta_{mu}$ . This is because all the STAs were allowed to engage in the MIMO phase and the same transmit antenna configuration was chosen for every SINR threshold. Table III presents the numerical and simulation results of the LSB scheme for a threshold  $\delta_{mu}$  value of 3. The results demonstrate that the duration times of the LSB scheme are much longer than those of the ILQE and LNS schemes. For each STA, the LSB scheme employed the best single beam (obtained from its SISO feedback) that could reach the STA with the highest SINR, without considering other STAs that it would have been able to reach at the same time; hence, the AP performed many unnecessary transmissions.

Next, with the low transmit power, i.e.,  $\rho = 2.5$  dBm and  $\sigma^2 = -85$  dBm, all the STAs were not always allowed to engage in the MIMO phase, as mentioned earlier in this section. Both the LSB and LNS schemes also excluded certain STAs from the MIMO phase if the SINRs of the single beams included in their SISO feedback were all lower than the threshold  $\delta_{mu}$ . Fig. 12(e) depicts that our ILQE scheme allowed a larger number of STAs to engage than the two comparison schemes. This is because our scheme considered the benefit of the transmit diversity gain and could identify a greater number of reachable STAs. As depicted in Fig. 12(e) and Figs. 12(a)–(d), the number of STAs that were engaged affected the duration of each subphase; the duration decreased in most cases as the threshold  $\delta_{mu}$  increased. Fig. 12(f) indicates that our ILQE scheme had the shortest duration when supporting the STA subgroups that were also supported by the

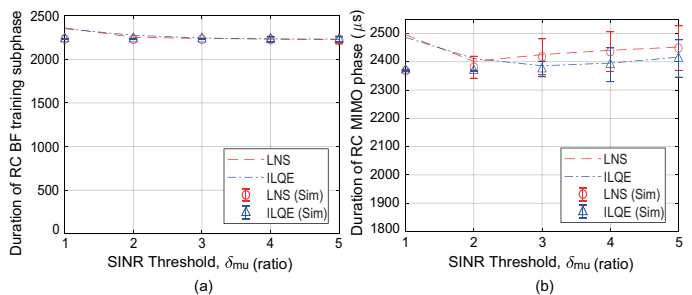


Fig. 11. Duration of the (a) RC BF training subphase and (b) RC MIMO phase when using high transmit power.

LNS and LSB schemes, i.e., in SCC. However, our scheme required additional duration time to support the subgroups that the comparison schemes were incapable of testing, i.e., in AAS.

### B. Performance of the RC MIMO Phase

The RC MIMO phase comprises the BF setup, training, and selection subphases. The BF setup and selection subphases of the RC MIMO phase are entirely the same as those of the NRC phase. However, the BF training subphase of the RC MIMO phase operates in the same manner as the BF feedback subphase of the NRC phase; hence, as depicted in Fig. 11(a) and Fig. 12(g), the duration of the BF training subphase mainly depends on the number of STAs engaging in the MIMO phase, as in Fig. 7(c) and Fig. 12(c), respectively.

Fig. 11(a) and 12(h) depict plots of the total duration of the RC MIMO phase with high and low transmit powers, respectively. Our ILQE scheme outperformed both the comparison schemes in terms of the BFT time, provided the same STAs engaged in the RC MIMO phase, i.e., in the SCC case. Moreover, our scheme was capable of supporting more STAs in the MIMO phase in comparison with the LSB and LNS schemes. Fig. 12(h) depicts that our scheme consumed slightly more BFT time than the existing schemes when it supported all the STAs engaging in the RC MIMO phase, i.e., in AAS.

### C. Channel Estimation Error and Computational Complexity

Our ILQE scheme estimates the channel vector of multiple beams by using the channel information corresponding to each single beam that is included in the SISO feedback. In this section, the actual and estimated channel vectors are represented as  $\mathbf{h}_{cir}$  and  $\hat{\mathbf{h}}_{cir}$ , respectively. The normalized mean squared error (NMSE) of the channel estimation is defined as  $E[(\|\mathbf{h}_{cir} - \hat{\mathbf{h}}_{cir}\|_2)^2] / E[(\|\mathbf{h}_{cir}\|_2)^2]$ . Fig. 13(a) shows the NMSEs measured when the high and low transmit powers were used. We observed that, on average, the NMSE was higher with a low transmit power; nevertheless, our ILQE scheme still outperformed the LNS and LSB schemes, as shown in Fig. 12. Although high NMSEs were measured for more STAs with the low transmit power compared with the high one, these STAs were mostly excluded from the BFT in all schemes (i.e., ILQE, LNS, and LSB) because the SINRs

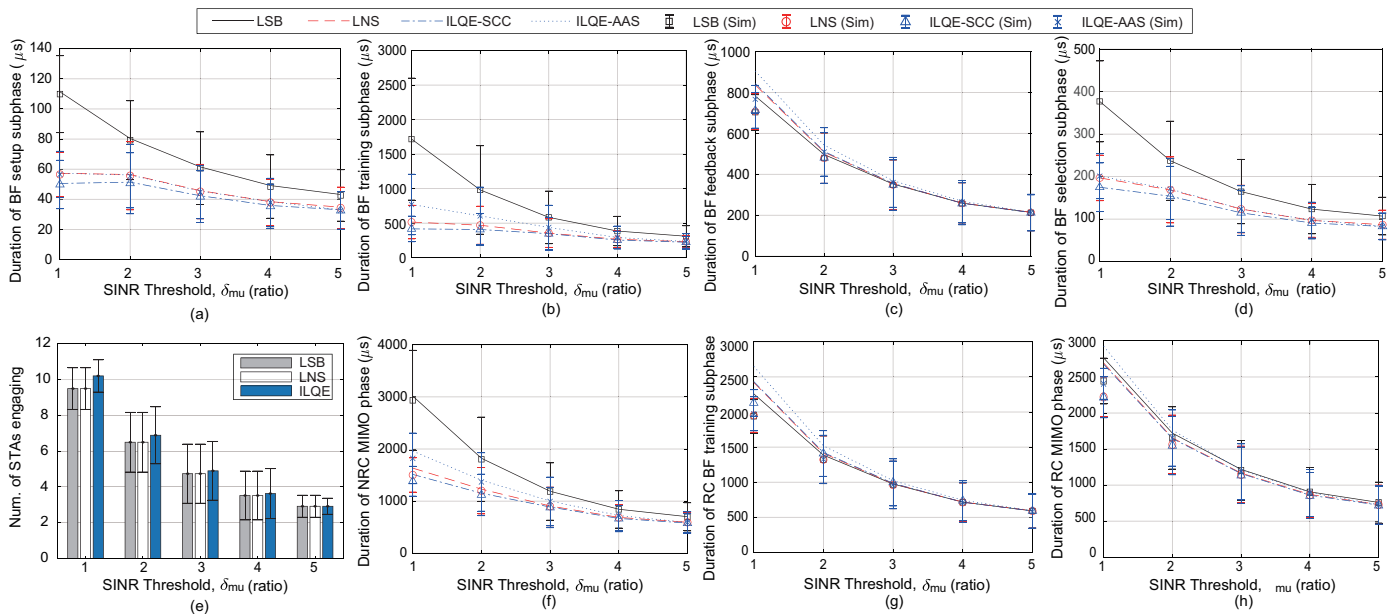


Fig. 12. Duration of (a) BF setup, (b) BF training, (c) BF feedback, and (d) BF selection subphases in the NRC MIMO phase, (e) number of STAs engaging in the MIMO phase, and duration of (f) the NRC MIMO phase, (g) RC BF training subphase, and (h) RC MIMO phase for low transmit power, i.e.,  $\rho = 2.5$  dBm and  $\sigma^2 = -85$  dBm.

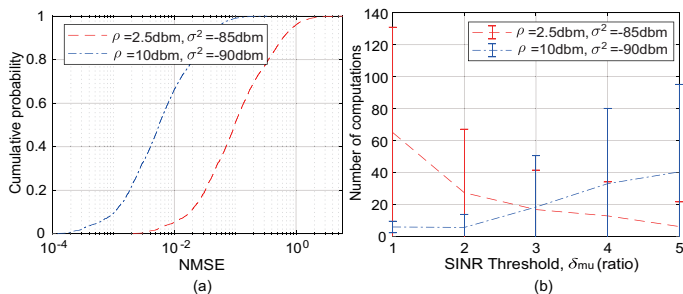


Fig. 13. (a) Channel estimation error, i.e., NMSE, and (b) the number of times the SINRs are computed in our ILQE scheme.

of the single beams included in their SISO feedback were all less than the SINR threshold,  $\delta_{mu}$ .

Fig. 13(b) plots the average number of times the SINRs were computed using Eq. (13) when our heuristic method was performed as described in Section III-D. As shown in the case of the high transmit power, the number of computations increased as the SINR threshold  $\delta_{mu}$  increased; this is because the SINR of each single beam, which was known from the SISO feedback, was more likely to be less than  $\delta_{mu}$ . However, with the low transmit power, the number of computations decreased as  $\delta_{mu}$  increased; this can be attributed to the number of STAs engaging in the BFT decreasing with an increase in  $\delta_{mu}$ .

## VI. CONCLUSION

The MU-MIMO BFT enables an AP and STAs in an MU group to determine the appropriate transmit and receive AWVs, respectively, for DL MU-MIMO transmission. However, if the AP is incapable of efficiently identifying STAs

within the reach of an action frame transmitted in the MU-MIMO BFT, it performs unnecessary transmissions, thereby increasing the BFT time. To reduce the BFT time, existing schemes employ multiple TSs simultaneously to transmit an action frame. However, these existing schemes ignore the transmit diversity gain resulting from the use of multiple TSs at a time.

In this study, we proposed an efficient transmit antenna configuration scheme capable of capturing the benefit of the transmit diversity, as well as the effect of ISI. The numerical and simulation results demonstrated that our ILQE scheme outperforms existing schemes in terms of the BFT time. The results also revealed that our ILQE scheme can perform the BFT with many different subgroups of STAs in the MU group, which is not supported by the existing schemes.

## REFERENCES

- [1] C. Chen, O. Kedem, C. R. C. M. da Silva and C. Cordeiro, "Millimeter-Wave Fixed Wireless Access Using IEEE 802.11ay," *IEEE Commun. Mag.*, vol. 57, no. 12, pp. 98-104, Dec. 2018.
- [2] *Enhanced Throughput for Operation in License-exempt Bands Above 45 GHz*, IEEE P802.11ay/D4.0, June. 2019.
- [3] Y. Ghasempour, C. R. C. M. da Silva, C. Cordeiro, and E. W. Knightly, "IEEE 802.11ay: Next-generation 60 GHz communication for 100 Gb/s Wi-Fi," *IEEE Commun. Mag.*, vol. 55, no. 12, pp. 186-192, Dec. 2017.
- [4] M-S. Kim, T. Ropitault, S.K. Lee, and N. Golmie, "Efficient MU-MIMO Beamforming Protocol for IEEE 802.11ay WLANs," *IEEE Commun. Lett.*, vol. 23, no. 1, pp. 144-147, Jan. 2019.
- [5] P. Zhou, K. Cheng, X. Fang, Y. Fang, R. He, Y. Long, and Y. Liu, "IEEE 802.11ay based mmWave WLANs: Design challenges and solutions," *IEEE Commun. Surv. Tutor.*, vol. 20, no. 3, pp. 1654-1681, Mar. 2018.
- [6] S. Blandino, G. Mangraviti, C. Desset, A. Bourdoux, P. Wambacq, and S. Pollin, "Multi-User Hybrid MIMO at 60 GHz Using 16-Antenna Transmitters," *IEEE Trans. Circuits and Systems-1*, vol. 66, no. 2, pp. 848-858, Feb. 2019.
- [7] Y. Ghasempour, M. K. Haider, and E. W. Knightly, "Decoupling Beam Steering and User Selection for MU-MIMO 60-GHz WLANs," *IEEE/ACM Trans. Networking*, vol. 26, no. 5, pp. 2390-2403, Oct. 2018.

- [8] Y. Ghasempour, M. K. Haider, and E. W. Knightly, "Multi-User Multi-Stream mmWave WLANs with Efficient Path Discovery and Beam Steering," *IEEE Journal on Selected Areas*, vol. 37, no. 2, pp. 2744-2758, Dec. 2019.
- [9] N. J. Myers, A. Mezghani, and R. W. Heath, Jr., "FALP: Fast beam alignment in mmWave systems with low-resolution phase shifters," *IEEE Trans. Commun.*, vol. 67, no. 12, pp. 8739-8753, Dec. 2019.
- [10] W. Wu, N. Cheng, N. Zhang, P. Yang, W. Zhuang, and X. Shen, "Fast mmwave beam alignment via correlated bandit learning," *IEEE Trans. Wireless Commun.*, vol. 18, no. 12, pp. 5894-5908, Dec. 2019.
- [11] H. Assasa, J. Widmer, T. Ropitault, and N. Golmie, "Enhancing the ns-3 IEEE 802.11ad Model Fidelity: Beam Codebooks, Multi-Antenna Beamforming Training, and Quasi-Deterministic mmWave Channel," in *Proc. Workshop Ns-3*, 2019.
- [12] X. Gao, L. Dai, S. Han, C.-L. I, and R. W. Heath, "Energy-efficient hybrid analog and digital precoding for mmWave MIMO systems with large antenna arrays," *IEEE Journal on Selected Areas*, vol. 34, no. 4, pp. 998-1009, Apr. 2016.
- [13] A.H. Mehana and A. Nosrantina, "Single-Carrier Frequency-Domain Equalizer with Multi-Antenna Transmit Diversity," *IEEE Trans. Wireless Commun.*, vol. 12, no. 1, pp. 388-397, Jan. 2013.
- [14] O.E. Ayach, S. Rajagopal, S. Abu-Surra, Z. Pi, and R.W. Heath, "Spatially Sparse Precoding in Millimeter Wave MIMO Systems," *IEEE Trans. Wireless Commun.*, vol. 13, no. 3, pp. 1499-1513, Mar. 2014.
- [15] E. Torkildson, U. Madhow, and M. Rodwell, "Indoor Millimeter Wave MIMO: Feasibility and Performance," *IEEE Trans. Wireless Commun.*, vol. 10, no. 12, pp. 4150-4160, Dec. 2011.
- [16] P. Kumari, J. Choi, N. G-Prelcic, and R. W. Heath Jr., "IEEE 802.11ad-Based Radar: An Approach to Joint Vehicular Communication-Radar System," *IEEE Trans. Veh. Technol.*, vol. 67, no. 4, pp. 3012-3027, Apr. 2018.
- [17] W-C. Liu, F-C. Yeh, T-C. Wei, C-D. Chan and S-J. Jou, "A Digital Golay-MPIC Time Domain Equalizer for SC/OFDM Dual-Modes at 60 GHz Band," *IEEE Trans. on Circuits and Systems*, vol. 60, no. 10, pp. 2730-2739, Oct. 2013.
- [18] D. Halperin, S. Kandula, J. Padhye, P. Bahl and D. Wetherall, "Augmenting Data Center Networks with Multi-Gigabit Wireless Links," in *Proc. ACM SigComm 2011*, vol. 41, no. 4, pp. 38-49, Aug. 2011.
- [19] *Channel Models for IEEE 802.11ay*, IEEE P802.11-15/1150r9, Mar. 2017.
- [20] A. Bodi, J. Zhang, J. Wang and C. Gentile, "Physical-Layer Analysis of IEEE 802.11ay based on a Fading Channel Model from Mobile Measurements," in *Proc. IEEE IEEE Int. Conf. Commun.*, May 2019.
- [21] C. D. Iskanderp, "A matlab-based object-oriented approach to multipath fading channel simulation," Mathworks, Natick, MA, Tech. Rep. 18869, Feb. 2008.
- [22] *A Collection of Open-source Tools to Simulate IEEE 802.11ad/ay WLAN Networks in ns-3*. <https://github.com/wigig-tools>